

# Changes in the N- and C-terminal sequences of the murine R7 Gag-tMos protein affect brain lesion induction

Pick-Hoong Yuen<sup>\*.1</sup>, Eric Devroe<sup>1</sup>, Kit-Yeng Lim<sup>1</sup> and Paul KY Wong<sup>1</sup>

<sup>1</sup>Department of Carcinogenesis, Science Park-Research Division, The University of Texas M.D. Anderson Cancer Center, PO Box 389, Smithville, Texas, TX 78957, USA

Our preliminary studies suggested that the novel *gag*-truncated *mos* (*tmos*) open reading frame (ORF) of R7, a spontaneous deletion mutant of Moloney murine sarcoma virus 124 (MoMuSV124), may be responsible for R7's unique ability to induce brain lesions in all R7-injected mice. However, when we replaced the *gag-tmos* ORF with either the MoMuSV124 or the homologous myeloproliferative sarcoma virus *env-mos* gene, we found that both recombinant viruses also induced brain lesions in all injected mice. Although these studies suggested that the critical determinants for brain lesion induction may reside in the *tmos* sequence common to all three viruses, they did not demonstrate if the N-terminus of Mos was dispensable for this activity. By inserting the FLAG sequence at the 3' end of the R7 *gag-tmos* ORF, we demonstrated that R7 does synthesize a Gag-tMos fusion protein. Using R7 *gag* deletion mutants with and without the FLAG sequence, we further demonstrated that (i) deletion of the entire *gag* sequence abolished R7's transforming activity; (ii) the ability of the virus to transform cultured NIH/3T3 cells was significantly reduced only when most of *gag* was deleted; (iii) the ability of the virus to induce brain lesions was inversely proportional to the extent of its *gag* deletions; and (iv) the insertion of FLAG at the Mos C-terminus did not reduce the *in vitro* transforming activity of the FLAG-tagged viruses but did reduce their ability to induce brain lesions. Thus, we have demonstrated that altering the N- or C-terminus of the R7 Gag-tMos fusion protein can affect disease manifestation. *Journal of NeuroVirology* (2000) 6, 329–340.

**Keywords:** brain; pathogenic; defective; FLAG-tagged; MoMuSV

## Introduction

The Moloney murine sarcoma virus (MoMuSV) family comprises *mos*-containing, acute transforming, replication-defective retroviruses. When injected into newborn mice, all known MoMuSV strains induce different types of subcutaneous sarcomas in mice (Moloney, 1966; Perk and Moloney, 1966; Chirigos *et al*, 1968; Stanton *et al*, 1968; Berman and Allison, 1969; Simons and McCully, 1970; Gazdar *et al*, 1972; Stoica *et al*, 1990; Yuen *et al*, 1991; Yuen and Kwak, 1997). Plasma-passaged sarcoma virus (SV-PP), a variant of MoMuSV obtained by animal passage, and its subclone, myeloproliferative sarcoma virus (MPSV), induce not only subcutaneous sarcomas but also myeloproliferation in mice (Chirigos *et al*, 1968; Le

Bousse-Kerdiles *et al*, 1980; Ostertag *et al*, 1980; Stoica *et al*, 1990; Yuen *et al*, 1991).

We have recently isolated R7, a spontaneously generated MoMuSV124 deletion mutant that induces not only sarcomas with a well-developed angiomatous component (fibroangiosarcomas), but also brain angioendotheliomas and brain hemorrhage (collectively referred to as brain lesions) (Yuen and Kwak, 1997, 1998). R7 is unique among known MoMuSVs in its ability to induce brain lesions in all mice injected intraperitoneally with a high titer of the virus. Previously, only two viruses were reported to possess this pathogenic ability: an uncharacterized MoMuSV strain that induces brain lesions at the site of inoculation when injected intracranially into rats (Ribacchi and Giraldo, 1966), and an uncharacterized isolate of MPSV that induces hemangiosarcomas exclusively in the cerebellum in 54% of intravenously injected new-

\*Correspondence: PH Yuen  
Received 29 December 1999; accepted 9 March 2000

born rats (Hayashi *et al*, 1988). More recently, transgenic mice carrying a *c-mos* or *v-mos* gene flanked by MSV m1 long terminal repeats (LTRs) have been reported to develop behavioral abnormalities and neurologic symptoms culminating in paralysis but, interestingly, no sarcomas (Propst *et al*, 1990, 1992).

Sequence analysis of the R7 genome indicates that the R7 genome differs structurally from the MoMuSV124 genome in several important ways (Yuen and Kwak, 1997). These differences include (i) incorporation of an additional direct repeat in the enhancer; (ii) deletion of most of the MoMuLV-derived *gag* sequence, all of the *pol* sequence, and the 15 bp N-terminal *env* sequence; (iii) deletion of the first 203 bp of the *mos* gene; and (iv) insertion of 7 bp generating a p15-p30-*tmos* ORF that likely results in the expression of a myristylated p15-p30-*tMos* fusion protein. We suspect that one or more of these structural changes alter the replication and transforming activity of R7 and thereby broaden R7's disease-inducing potential to include the induction of brain lesions.

Although R7 and MoMuSV124 share identical LTRs (except for an additional direct repeat in each R7 LTR), as well as 5' and 3' noncoding sequences, MoMuSV124 does not induce brain lesions. Furthermore, our preliminary experiments indicated that an R7 virus containing only two direct repeats, as found in MoMuSV124, also induces brain lesions (unpublished results). These findings suggest that the in-frame R7 *gag-tmos* sequence encoding a Gag-*tMos* protein may be responsible for the broadened disease potential of R7. To test this possibility, we substituted the R7 *gag-tmos* ORF and the adjacent 53 bp of the 5' noncoding sequence with either the MoMuSV124 or MPSV *env-mos* oncogene generating SV7d1 and SVM1, respectively. R7 *tMos* is identical to residues 69–374 of the SV7d1 Env-Mos fusion protein. The first five residues of the SV7d1 N-terminal 68 residues are the first five residues of the Env protein. SVM1 also encodes a homologous Env-Mos fusion protein, but differs from SV7d1 Env-Mos in 16 residues, 14 of which are found in the sequence commonly shared with SV7d1 and R7. Thus, if R7 encodes a Gag-*tMos* fusion protein, then R7 has substituted the 68 N-terminal Env-Mos residues of SV7d1 and SVM1 with 151 residues consisting of 146 residues encoded by p15 and p30 and five residues unique to the R7 genome (Yuen and Kwak, 1997). We demonstrated that both SV7d1 and SVM1 also induce brain lesions in all injected mice (Lim *et al*, 2000). However, angioendotheliomas induced by SV7d1 and especially SVM1 consist of markedly fewer abnormally enlarged endothelial cells (ECs) than do those induced by R7.

The above findings indicate that the Mos N-terminal residues 1–68 of MoMuSV124 (or the corresponding residues of MPSV Mos) and the Gag

residues of R7 (including the five residues unique to R7) can be interchanged without loss of the transforming activity leading to brain lesion induction. Since R7, SV7d1, and SVM1 have identical genetic backgrounds, differences in their Mos proteins may be responsible for their differential effects on brain ECs. One could infer that the residues of R7 *tMos*, and the corresponding residues of SV7d1 and SVM1 Env-Mos, contain all the essential elements required for transformation of brain ECs. However, the above findings did not demonstrate that the N-terminal Mos sequence is dispensable for transforming activity *in vitro* or induction of brain lesions *in vivo*. Therefore, in the present study, we sought to determine if the N-terminal sequence of Mos is dispensable for the Mos activity necessary for brain lesion induction by determining if (i) R7 in fact synthesizes a Gag-*tMos* protein as deduced from its nucleotide sequence; (ii) deletion of the entire R7 *gag* sequence affects R7's transforming activity *in vitro*; (iii) partial deletion of the R7 *gag* sequence affects R7's ability to transform cultured fibroblasts and induce brain lesions in BALB/c mice; and (iv) insertion of the FLAG sequence at the Mos C-terminus affects the virus's ability to transform cultured fibroblasts or induce brain lesions in BALB/c mice.

## Results

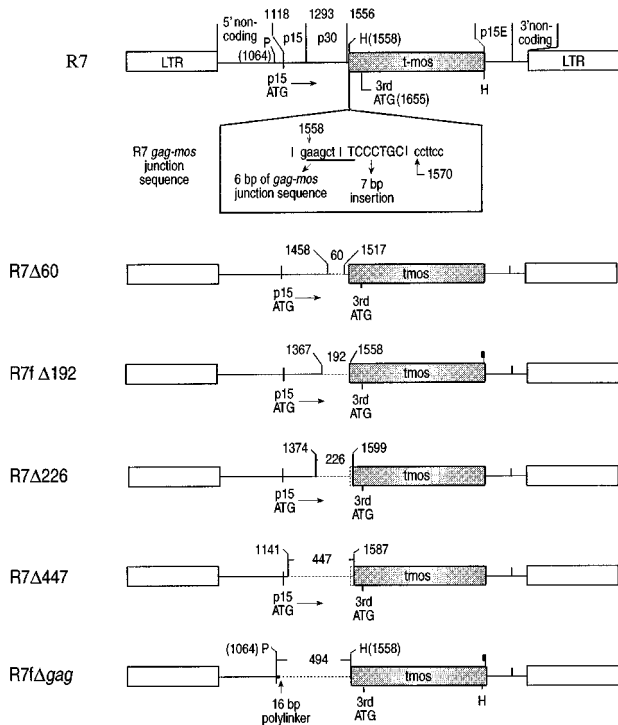
### Constructs

Figure 1 illustrates the panel of viruses used in this study. The construction of these viruses is described in Materials and methods.

### Synthesis of a Gag-*tMos* fusion protein by FLAG-tagged R7 (R7f)

To determine if R7 synthesizes a Gag-*tMos* fusion protein, we inserted the FLAG sequence at the 3' end of the R7 *tmos* gene immediately before the stop codon (Figure 2). The FLAG epitope is recognized by the M2 antibody (Sigma, St. Louis, MO, USA). The insertion of FLAG was necessary because residues 37–55 of the MoMuSV124 Mos protein, which are specifically recognized by the most effective Mos antibody (37–55) (Gallick *et al*, 1985), are deleted in R7 (Yuen and Kwak, 1997).

The M2 antibody detected a unique protein (Figure 3A, lane 4) in R7f-infected NIH/3T3 cells but not in R7-infected (lane 3) or uninfected NIH/3T3 cells (lane 2). On the basis of its mobility in five experiments, the average molecular mass of the protein detected only in the R7f-infected lysate was determined to be ~54 kDa, which is very similar to the molecular mass deduced from the R7 *gag-tmos* ORF (Table 1). Addition of the FLAG peptide eliminated the 54-kDa band (Figure 3A, lane 5), which verified that the 54-kDa protein contained the FLAG epitope. The additional bands observed in lanes 2–4 were also eliminated in the presence of



**Figure 1** R7 and its gag deletion mutants. Details of their construction are described in Materials and methods. Solid lines, sequences common to the genomes; dotted lines, deleted sequences; numbers, position of specific segments of the R7 genome except for the numbers above dotted lines, which represent the number of bp deleted; open box, R7 LTR; filled box, R7 tmos coding sequence; H, *HindIII*; P, *PstI*; underlined, *HindIII*.



**Figure 2** Insertion of the FLAG sequence at the 3' end of the mos coding sequence. Numbers below sequence denote position of the base pairs in the R7 genome. The FLAG coding sequence is in lowercase letters, the termination codon is underlined, and the *HindIII* site is boxed.

FLAG peptide, which suggests that these were nonspecific epitopes recognized by the M2 antibody. In addition, the 54-kDa protein was also detected using a monoclonal antibody against CasBrE MLV p15 (Figure 3B, lane 3). The additional bands likely corresponded to Pr27<sup>gag</sup> (p15–p12), Pr55<sup>gag</sup>, and Pr65<sup>gag</sup> expressed by the helper virus, MoMuLV-TB. The additional ~76 kDa band remains unidentified. The above findings demonstrated that R7f synthesized a Gag-tMos fusion protein as predicted from its nucleotide sequence.

Additional experiments indicated that maximum expression of the R7f Gag-tMos protein peaked at 4 days and was markedly reduced 12 days after *de novo* infection (data not shown).

#### Synthesis of Gag-tMos fusion proteins by R7fΔ60, R7fΔ192 and R7fΔ447

We constructed R7fΔ60, R7fΔ192 and R7fΔ447 as described in Materials and methods. Western blot analysis of R7fΔ60-, R7fΔ192-, and R7fΔ447-infected NIH/3T3 cell lysates was performed to determine if these viruses also synthesized Gag-tMos proteins. FLAG-tagged proteins of ~51 (Figure 4, lane 5), ~44 (lane 6), and ~36 kDa (lane 7), respectively, were detected. The observed molecular masses of R7fΔ60 and R7fΔ447 were slightly higher than predicted by their respective gag-tmos ORFs, while the observed molecular mass of R7fΔ192 was slightly lower than predicted (Table 1). A slight discrepancy between the observed and predicted molecular mass of the MoMuSV124 protein has been previously observed (Herzog et al, 1990). Therefore, like R7f, R7fΔ60, R7fΔ192, and R7fΔ447 also synthesized Gag-tMos fusion proteins.

#### Inability of R7fΔgag to transform NIH/3T3 cells or synthesize a tMos protein

To determine if the entire gag sequence of R7 is dispensable for transforming activity, we constructed deletion mutant R7fΔgag in which the whole R7f gag sequence was deleted (Figure 1, line 6), as described in Materials and methods.

Although G418-resistant colonies were obtained when R7fΔgag and pUCNeo DNAs were coelectroporated into Ψ2 cells and grown in G418-containing medium, none of them were transformed. Nevertheless, a polymerase chain reaction (PCR) product diagnostic of the R7fΔgag genome was obtained from DNA extracted from pooled G418-resistant colonies (data not shown). NIH/3T3 cells infected with a large volume of the supernatant from the above G418-resistant Ψ2 cells remained untransformed. The infected NIH/3T3 cells were single-cell cloned. Screening of 20 single-cell clones by PCR amplification using primer sets ms51-ms32 and L5-ms32 identified two single-cell clones containing the R7fΔgag genome. These R7fΔgag-infected single-cell clones were designated R7fΔgagSc1 and R7fΔgagSc2. These cell lines were also untransformed. Nevertheless, a single mos-specific RNA transcript was detected when total RNA from R7fΔgagSc1 cells was analyzed (Figure 5A, lane 1), indicating that the viral RNA (vRNA) served as both messenger and genomic RNA. The deduced size of this transcript was 2.2 kb. In addition, R7fΔgagSc1 cells superinfected with MoMuLV-TB remained untransformed, although R7fΔgag vRNA was detected in particles pelleted from the supernatant of the R7fΔgagSc1 cells superinfected with MoMuLV-TB (Figure 5A, lane 2). Despite the above

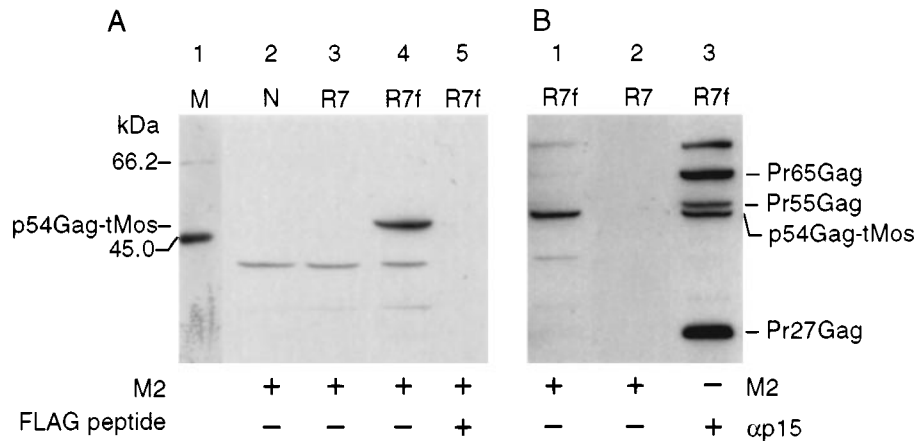


**Figure 3** Western blots of uninfected, R7-, or R7f-infected NIH/3T3 cell lysates. (A) Protein lysates (20  $\mu$ g each) were fractionated and probed with 2  $\mu$ g/ml M2 antibody (lanes 2–4) or 2  $\mu$ g/ml M2 antibody pretreated with 16.6  $\mu$ g/ml FLAG peptide (lane 5). M, broad-range biotinylated marker, N, uninfected NIH/3T3 cells. (B) Protein lysates (20  $\mu$ g each) were fractionated and probed with 2  $\mu$ g/ml M2 antibody (lanes 1–2) or undiluted monoclonal antibody to CasBrMLV p15 (lane 3) as described in Materials and methods.

**Table 1** Deduced versus actual molecular masses of Gag-tMos and tMos proteins

Genome	Predicted no. of residues in Gag-tMos or tMos proteins	Deduced molecular mass of Gag-tMos or tMos proteins (kDa) <sup>a</sup>	Molecular mass of Gag-tMos proteins detected by Western blotting (kDa) <sup>b</sup>
R7f	466	52.1	53.7
R7f $\Delta$ 60	446	49.6	51.4
R7f $\Delta$ 192	401	44.7	43.6
R7 $\Delta$ 447	316	34.9	36.0
R7f $\Delta$ gag	286 <sup>c</sup>	31.5	nd <sup>d</sup>

<sup>a</sup>Based on the molecular mass of the predicted amino acid sequence. <sup>b</sup>Reported value represents the mean value obtained from five separate experiments. <sup>c</sup>Assuming translation is initiated at the third ATG of the MoMuSV124 *env-mos* sequence (which is the first ATG within the *tmos* sequence). <sup>d</sup>nd, none detected.

findings, no FLAG-tagged tMos protein was detected in NIH/3T3 cells infected *de novo* with a large volume of R7f $\Delta$ gagSc1+MoMuLV-TB supernatant (Figure 5B, lane 3). Together, these findings demonstrated that the R7f $\Delta$ gag virus was produced but failed to transform NIH/3T3 cells. Therefore, in order for R7 to transform fibroblasts *in vitro*, the entire *gag* sequence cannot be deleted.

#### Importance of the R7 Gag residues forming the N-terminus of R7 Gag-tMos fusion protein

To determine how much of the *gag* sequence is required for the transformation of cultured fibroblasts and the induction of brain lesions, we constructed the R7 *gag* deletion mutants R7 $\Delta$ 60, R7 $\Delta$ 226, and R7 $\Delta$ 447 and compared them with R7 in terms of their transforming and transcriptional activities in NIH/3T3 cells and their abilities to induce brain lesions in BALB/c mice.

**Transforming activity of R7 and its *gag* deletion mutants** The transforming activities of R7, R7 $\Delta$ 60, R7 $\Delta$ 226, and R7 $\Delta$ 447 were assayed using the NIH/3T3 focus-forming assay. This assay also measures a virus's replication efficiency, provided

the transforming activity of the virus is unimpaired. To compare the transforming activity of the viruses, the supernatants from several cell lines chronically infected with R7 or one of its *gag* deletion mutants were assayed. To confirm the results obtained from chronically infected cells, NIH/3T3 cells were also infected *de novo* with R7, R7 $\Delta$ 60, R7 $\Delta$ 226, or R7 $\Delta$ 447 at a multiplicity of infection (m.o.i.) of 5. The supernatants from these *de novo* infections were also assayed. In both cases, the number of focus forming units (FFUs) detected was normalized to the number of FFUs produced by 10<sup>6</sup> cells in 1 ml of supernatant over a 24-h period. The results obtained are shown in Figure 6.

Statistical analysis indicated that the number of R7, R7 $\Delta$ 60, and R7 $\Delta$ 226 FFUs produced did not significantly differ (in either chronic or *de novo* infections). However, chronic and *de novo* infections with R7 $\Delta$ 447 produced significantly fewer FFUs than did similar infections with R7, R7 $\Delta$ 60, or R7 $\Delta$ 226 ( $P < 0.01$ ).

**Transcriptional activity of R7 and its *gag* deletion mutants** To determine if the reduced number of

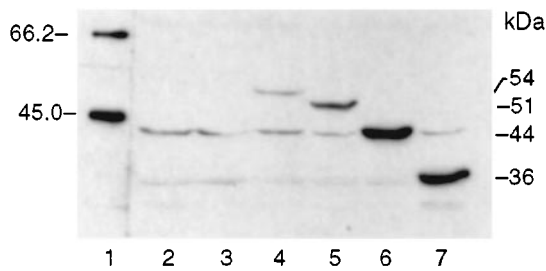


**Figure 4** Comparison of Gag-tMos protein synthesized by R7f and its *gag* deletion mutants. Protein lysates (20  $\mu$ g each) of uninfected (lane 2), R7-infected (lane 3), R7f-infected (lane 4), R7 $\Delta$ 60-infected (lane 5), R7 $\Delta$ 192-infected (lane 6), and R7 $\Delta$ 447-infected (lane 7) NIH/3T3 cells were fractionated and probed with 2  $\mu$ g/ml M2 antibody as described in Materials and methods. Lane 1, broad-range biotinylated protein marker.

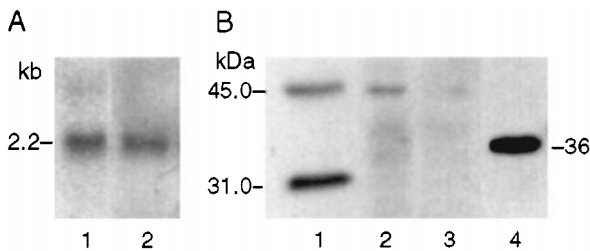


**Figure 5** RNA and protein synthesized by R7f $\Delta$ gag. (A) Northern blot: 5  $\mu$ g of total RNA isolated from R7f $\Delta$ gagSc1 cells (NIH/3T3 cells infected with R7f $\Delta$ gag only) (lane 1) or vRNA from virions pelleted from the supernatant of R7f $\Delta$ gagSc1 cells coinfecting with MoMuLV-TB (lane 2) was fractionated, transferred, and probed as described in Materials and methods. (B) Western blot: Lane 1, broad-range biotinylated protein markers; lanes 2–4, protein lysate (20  $\mu$ g each) of uninfected NIH/3T3 cells (lane 2), NIH/3T3 cells 3 days after infection with (i) 10 ml of supernatant harvested from R7f $\Delta$ gagSc1 cells coinfecting with MoMuLV-TB (lane 3), or (ii) R7 $\Delta$ 447 and MoMuLV-TB at an m.o.i. of 5 (lane 4). Membranes were probed with 2  $\mu$ g/ml M2 antibody as described in Materials and methods.

FFUs produced by R7 $\Delta$ 447 relative to R7, R7 $\Delta$ 60, and R7 $\Delta$ 226 was due to reduced transcriptional activity of this *gag* deletion mutant, total RNA was extracted and analyzed by Northern blotting, as described in Materials and methods. A single RNA transcript was detected from each infected cell line (Figure 7B) when total RNA (Figure 7A) was probed with a *mos*-specific probe. Thus, as previously noted for R7f $\Delta$ gag, the viral RNA appeared to serve as both messenger and genomic RNA. The size of the transcript decreased as the number of bp deleted increased. The approximate size of the R7, R7 $\Delta$ 60, R7 $\Delta$ 226, and R7 $\Delta$ 447 RNA transcripts (deduced from their genomes) was 2.8 kb, 2.7 kb, and 2.3 kb, respectively. As shown in Figure 7, all viruses transcribed equivalent amounts of RNA, except for R7 $\Delta$ 447 which transcribed more RNA than did R7. Thus, the pronounced reduction in the number of FFUs produced by R7 $\Delta$ 447 was not due to reduced transcriptional activity.

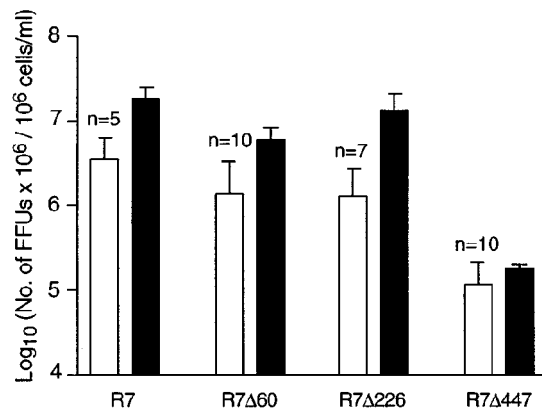


**Figure 6** Number of FFUs produced by R7 and its *gag* deletion mutants in chronically infected cell lines and in *de novo* infections. The transforming activity of R7 or one of its *gag* deletion mutants produced by chronically infected cell lines (open bars) or in *de novo* infections (filled bars) was determined as described in Materials and methods. The open bars represent the mean number of FFUs produced by several (*n*) chronically infected cell lines. The filled bars represent the mean number of FFUs obtained from two or more independent assays of the same 24-h supernatant harvested 4 d.p.i. Error bars, standard deviation.

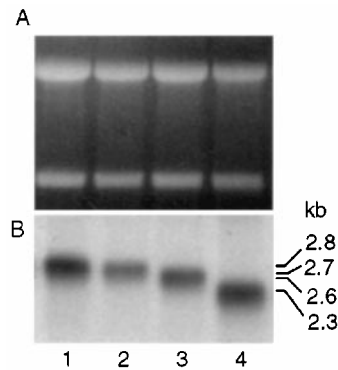


**Figure 7** Comparison of the amounts of *mos*-specific RNA synthesized by R7 and its *gag* deletion mutants. NIH/3T3 cells seeded into 60-mm plates were infected with R7, R7 $\Delta$ 60, R7 $\Delta$ 226, or R7 $\Delta$ 447 at an m.o.i. of 5. Three days later, the infected cells were transferred into 100-mm plates. RNA was extracted when the cells were confluent. (A) Total RNA (3  $\mu$ g each) was fractionated and stained with ethidium bromide as described in Materials and methods. (B) The gel shown in (A) was transferred and probed with a *mos*-specific probe as described in Materials and methods. Lane 1, R7; lane 2, R7 $\Delta$ 60; lane 3, R7 $\Delta$ 226; lane 4, R7 $\Delta$ 447. The RNA transcript sizes deduced from the respective genomes are indicated.

**Brain lesion-inducing ability of R7 and its *gag* deletion mutants** Previously, we reported that the number of R7 FFUs injected affected both the incidence and number of brain lesions induced in mice (Yuen and Kwak, 1998). The data in Table 2 include previously published results for R7-infected mice (Yuen and Kwak, 1998). The combined results of our studies showed that all mice injected with  $4 \times 10^5$  FFUs or more developed brain lesions.

**Table 2** Incidence of brain lesions induced by R7 and its gag deletion mutants<sup>a</sup>

Virus	No. of FFUs × 10 <sup>5</sup> injected	No. of mice injected	Mean latent period (days)	Incidence of brain lesions (%)	Severity of brain lesions <sup>b</sup>
R7	4-40	20	19	100	+++
	2-3	23	36	39	++
R7Δ60	5-25	36	32	53	+
	2-4	43	42	7	+
R7Δ226	5-10	37	39	35	+
R7Δ447	1-2	27	60	0	

<sup>a</sup>BALB/c mice less than 48 h old were injected intraperitoneally with FFUs in the range indicated. Mice were killed when moribund, except for R7Δ447-infected mice which remained healthy at 60 d.p.i. The experiment was terminated at 60 d.p.i. to avoid complications resulting from the onset of T-cell lymphoma induced by the helper virus MoMuLV-TB (which occurs about 4 months after injection). <sup>b</sup>+++ , > 50% of brains examined had >5 lesions; ++, >50% of brains examined had 3–5 lesions; +, >50% of brains examined had <3 lesions.

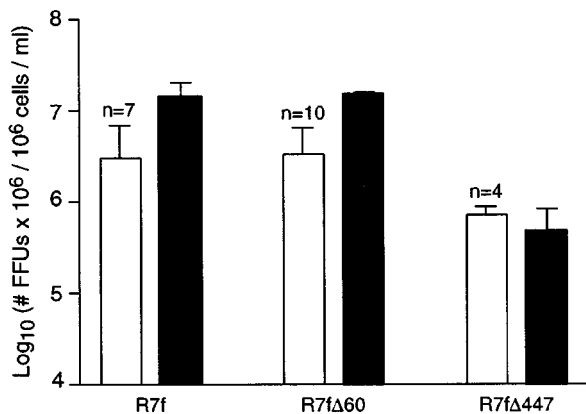


**Figure 8** Number of FFUs produced by R7f and its gag deletion mutants in chronically infected cell lines and in *de novo* infections. The transforming activity of R7f or one of its gag deletion mutants produced by several chronically infected cell lines (open bars) or in *de novo* infections (filled bars) was determined as described in Materials and methods. The open bars represent the mean number of FFUs produced by several (*n*) chronically infected cell lines. The filled bars represent the mean number of FFUs obtained from two or more independent assays of the same 24-h supernatant harvested 4 d.p.i. Error bars, standard deviation.

When mice were injected with  $2-3 \times 10^5$  R7 FFUs, the incidence of brain lesions decreased from 100 to 39%. Since all mice injected with  $4 \times 10^5$  R7 FFUs or more developed brain lesions, to compare the incidence of brain lesions induced by the panel of viruses, mice were injected with each gag deletion mutant, except for R7Δ447, in a similar range of FFUs. R7Δ447 was injected with the maximum titer obtained as determined by the NIH/3T3 cell focus forming assay. As shown in Table 2, R7Δ60 induced significantly fewer brain lesions (53%) than did R7 (100%) when greater than  $4 \times 10^5$  FFUs were

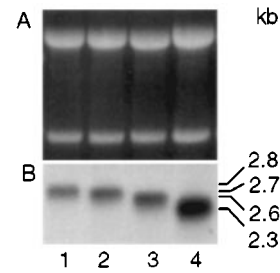


**Figure 9** Comparison of *mos*-specific RNA synthesized by R7f and its gag deletion mutants. NIH/3T3 cells were infected with R7f, R7fΔ60, R7fΔ192, or R7fΔ447. The experiment was performed as described in the legend to Figure 7. (A) Total RNA (3 μg each) was fractionated and stained with ethidium bromide as described in Materials and methods. (B) The gel shown in (A) was transferred and probed with a *mos*-specific probe as described in Materials and methods. Lane 1, R7f; lane 2, R7fΔ60; lane 3, R7fΔ192; lane 4, R7fΔ447. The RNA transcript sizes deduced from the respective genomes are indicated.

**Table 3** Incidence of brain lesions induced by R7f and its gag deletion mutants<sup>a</sup>

Virus	No. of FFUs × 10 <sup>5</sup> injected	No. of mice injected	Mean latent period (days)	Incidence of brain lesions (%)	Severity of brain lesions <sup>b</sup>
R7f	6-40	70	32	46	+
R7fΔ60	6-20	43	30	28	++
R7fΔ447	4-8	37	57	3	+

<sup>a</sup>BALB/c mice less than 48 h old were injected intraperitoneally with FFUs in the range indicated. Mice were killed when moribund, except for R7fΔ447-infected mice which remained healthy at 60 d.p.i. The experiment was terminated at 60 d.p.i. to avoid complications resulting from the onset of T-cell lymphoma induced by the helper virus MoMuLV-TB (which occurs about 4 months after injection). <sup>b</sup>+++ , > 50% of brains examined had >5 lesions; ++, >50% of brains examined had 3–5 lesions; +, > 50% of brains examined had <3 lesions.

injected ( $P < 0.0001$ ). The incidence of brain lesions was also significantly reduced when mice were injected with a lower range ( $2-4 \times 10^5$ ) of R7Δ60 FFUs compared to mice injected with a similar range ( $2-3 \times 10^5$ ) of R7 FFUs ( $P < 0.01$ ). In addition, R7Δ60-infected brains contained fewer lesions than did R7-infected brains and the latent period required for brain lesion induction was longer in R7Δ60-infected mice than in R7-infected mice.

The above findings clearly showed that, at both higher and lower dosages, deletion of 60 bp of the *gag* sequence significantly reduced the incidence and number of brain lesions. Thus, R7Δ60 is less virulent than R7. Table 2 also showed that R7Δ226 induced a significantly lower incidence of brain lesions (35%) than did R7 ( $P < 0.0001$ ), that brain lesions induced by R7Δ226 were also less severe than those induced by R7, and that R7Δ447 did not induce any brain lesions. Therefore, the ability of

**Table 4** Primers utilized for PCR amplification and sequencing

Name of primer	Nucleotide sequence	Position of bp in R7 genome <sup>a</sup>
L5	5'-AATGAAAGACCCCACCTGTAGG-3'	2–23
ms52as	5'-TTCAGGTCCTTGGGGCACCCCTGGA-3'	390–414 and 3125–3149
ms51	5'-CAGTCCCGCCTCCGTCTGAATTT-3'	997–1020
ms32	5'-TTCCCAGTCTATGGAGAACCAGGC-3'	1619–1642
ms32as	5'-GCCTGGTTCTCCATAGACTGGGAA-3'	1619–1642
ms34	5'-TGGCAATCTCTCCTTTTAGGA-3'	2199–2219
ms34as	5'-TCCTAAAAGGAGAGATTGCCCA-3'	2199–2219
FR <sup>b</sup>	5'-AAACAAAAGCTTTCACTTGTTCATCGTCGTCCTTGTAGTCGCC- TAGTCCCTCGGAAAGCC-3'	

<sup>a</sup>According to (Yuen and Kwak, 1997). <sup>b</sup>The FLAG coding sequence (Figure 2) is underlined.

the viruses to induce brain lesions was inversely proportional to the extent of their *gag* deletions.

#### Effects of FLAG insertion

To determine the effect of the insertion of FLAG at the 3' end of the *mos* gene, the transforming activities, the transcriptional activities, and the abilities of R7f, R7fΔ60, and R7fΔ447 to induce brain lesions were compared.

**Transforming activity of R7f and its *gag* deletion mutants** The transforming activities of R7f, R7fΔ60, and R7fΔ447 were assayed in NIH/3T3 cells as described in Materials and methods. The results obtained are shown in Figure 8. In both chronic and *de novo* infections, similar numbers of R7f and R7fΔ60 FFUs were produced. When the numbers of FFUs produced by R7f and R7fΔ60 were compared with the numbers of FFUs produced by R7 and R7Δ60, respectively, no statistically significant difference was observed in either chronic or *de novo* infections. Therefore, the insertion of FLAG in R7f and R7fΔ60 did not significantly alter their transforming activity. In contrast, in both chronic and *de novo* infections, R7fΔ447 produced significantly fewer FFUs than did R7f and R7fΔ60 ( $P < 0.01$ ). The significant reduction in the number of FFUs produced by R7fΔ447 versus R7f was consistent with the previously observed reduction in the number of FFUs produced by R7Δ447 versus R7. Interestingly, R7fΔ447 produced significantly more FFUs than did R7Δ447 ( $P < 0.01$ ) in chronically infected cell lines, although this difference was not observed in *de novo* infections. This discrepancy was likely due to the relative difference in the number of chronically infected R7Δ447 and R7fΔ447 cell lines assayed.

**Transcriptional activity of R7f, R7fΔ60, R7fΔ192, and R7fΔ447** NIH/3T3 cells were infected *de novo* with R7f, R7fΔ60, R7fΔ192, or R7fΔ447 at an m.o.i. of 5. As previously observed for R7 and its *gag* deletion mutants, when an equal amount of total RNA from each infected cell line (Figure 9A) was probed with a *mos*-specific probe, a single RNA transcript corresponding in size to each virus's

genome was detected (Figure 9B). As shown in Figure 9B, R7f, R7fΔ60, and R7fΔ192 transcribed similar amounts of RNA, but R7fΔ447 transcribed more RNA than did R7f. Thus, the significant reduction in the number of FFUs produced by R7fΔ447 was not due to reduced transcriptional activity.

**Brain lesion-inducing ability of R7f and its *gag* deletion mutants** As shown in Table 3, all mice injected with R7f or R7fΔ60 became moribund by 30–32 days post-infection (d.p.i.). By contrast, all but one mouse injected with R7fΔ447, remained healthy when euthanized at 60–65 d.p.i. Interestingly, the insertion of FLAG appeared to reduce the brain-lesion inducing potential of the viruses. The insertion of FLAG in R7 (R7f) significantly reduced the incidence of brain lesions ( $P < 0.0001$ ). Similarly, the insertion of FLAG in R7Δ60 (R7fΔ60) significantly reduced the incidence of brain lesions ( $P < 0.025$ ). Only one of 37 R7fΔ447-infected mice developed brain lesions. The data summarized in Table 3 also indicated that the ability of the FLAG-tagged viruses to induce brain lesions was inversely proportional to the extent of their *gag* deletion. These findings paralleled the results obtained for R7 and its *gag* deletion mutants (Table 2).

## Discussion

By inserting the FLAG sequence at the 3' end of the *gag-tmos* ORF, the present study demonstrated that R7 and its *gag* deletion mutants synthesized Gag-tMos fusion proteins. Furthermore, studies on the laboratory-generated R7fΔ*gag* virus in which the entire R7 *gag* sequence was deleted demonstrated that, even though R7fΔ*gag* virions were produced, they did not transform NIH/3T3 cells. Since FLAG-tagged tMos protein was not detected in NIH/3T3 cells freshly infected with R7fΔ*gag* particles, this indicates that initiation of tMos translation at the third methionine of MoMuSV124 Mos (which is the first AUG codon present in the *tmos* coding sequence) either did not occur or was extremely inefficient. This observation is consistent with the

finding that the context of the AUG codon is one of the factors influencing the fidelity and efficiency of the initiation of translation of eukaryotic mRNA (Kozak, 1987). Based on Kozak's findings, the context of the first and second MoMuSV124 AUGs is optimal for initiation of translation, while the context of the third AUG is not.

Studies of R7, its *gag* deletion mutants R7 $\Delta$ 60 and R7 $\Delta$ 447, and their FLAG-tagged counterparts indicated that only the transforming activity of R7 $\Delta$ 447 and R7f $\Delta$ 447 in NIH/3T3 cells was significantly different from that of R7 and R7f, respectively. Nevertheless, the incidence of brain lesions induced by R7, R7 $\Delta$ 60, and R7 $\Delta$ 447 decreased as the extent of the *gag* deletion increased (Table 2). A similar trend was also observed for their FLAG-tagged counterparts, R7f, R7f $\Delta$ 60 and R7f $\Delta$ 447 (Table 3). Only in the case of R7 $\Delta$ 447 and R7f $\Delta$ 447 did the loss in brain lesion-inducing ability correlate with a loss in *in vitro* transforming activity.

In the case of R7 $\Delta$ 447 and R7f $\Delta$ 447, one could argue that the reduced number of FFUs produced by chronic and *de novo* infected NIH/3T3 cells indicates the reduced replication efficiency of these viruses. This, in turn, could reduce their ability to induce brain lesions. To evaluate this possibility, we compared the genomes of all viruses studied. We found that, first, all viruses shared a common genetic background including identical LTRs, 5' noncoding sequence (containing the packaging and dimerization signal), and 3' noncoding sequence. Therefore, it is unlikely that R7 $\Delta$ 447 or R7f $\Delta$ 447 differed from the other viruses in their ability to transcribe their respective genomes or to perform the initial processes of virion assembly. Second, since the same helper virus (MoMuLV-TB) supplied the structural proteins, it is also unlikely that the deletion mutants were differentially impaired in assembly or adsorption. Finally, since all of the viruses utilized the p15 Met codon, as indicated by the size of their Gag-tMos proteins, it is likely that the initiation of translation for each Gag-tMos protein occurred with the same efficiency.

Moreover, our findings showed that when NIH/3T3 cells were infected with R7, R7 $\Delta$ 60, R7 $\Delta$ 226, or R7 $\Delta$ 447 at the same m.o.i., R7-, R7 $\Delta$ 60-, and R7 $\Delta$ 226-infected cells synthesized about the same amounts of *mos*-specific RNA, while R7 $\Delta$ 447-infected cells synthesized more *mos*-specific RNA (Figure 7B). Similar results were obtained when NIH/3T3 cells were infected with the FLAG-tagged counterparts R7f, R7f $\Delta$ 60, or R7 $\Delta$ 447 (Figure 9B). Together, these findings support our prediction that the transcriptional activity of the *gag* deletion mutants should not be impaired. In fact, we suggest that the increased amount of *mos*-specific RNA detected in R7 $\Delta$ 447- and R7f $\Delta$ 447-infected cells was due to the higher m.o.i. of R7 $\Delta$ 447 or R7f $\Delta$ 447 used than in other infections. We suggest that this has

arisen because of the reduced transforming activities of R7 $\Delta$ 447 and R7f $\Delta$ 447. Consequently, their titers as determined by the NIH/3T3 assay were underestimated. In light of the above findings, it is therefore unlikely that any of the viruses we studied actually differed in replication efficiency. In addition, it is likely that R7 $\Delta$ 447 and R7f $\Delta$ 447 had reduced transforming activity.

The present study also showed that the *in vitro* transforming activity of R7 $\Delta$ 60 and R7f $\Delta$ 60 in NIH/3T3 cells did not significantly differ from that of R7 and R7f, respectively. However, despite this similarity, the abilities of these two *gag* deletion mutants to induce brain lesions were significantly reduced when compared with those of R7 and R7f, respectively. To reconcile this apparent incongruity, we suggest that the NIH/3T3 cell focus-forming assay was not sufficiently sensitive to discriminate slight differences in the transforming potential between either the R7 and R7 $\Delta$ 60 or the R7f and R7f $\Delta$ 60 Gag-tMos proteins. In the case of R7 $\Delta$ 447 and R7f $\Delta$ 447, we suspect that the transforming activities of the R7 $\Delta$ 447 and R7f $\Delta$ 447 Gag-tMos proteins were more severely impaired than those of R7, R7 $\Delta$ 60 or their FLAG-tagged counterparts. We postulate that more than one R7 $\Delta$ 447 or R7f $\Delta$ 447 virion was required to induce an NIH/3T3 cell focus, which would drastically reduce the number of foci observed in the assay. In light of the above arguments, the ability of the *gag* deletion mutants to transform NIH/3T3 cells would not necessarily reflect their actual transforming activity. Therefore, it is likely that the significantly reduced incidence of brain lesions induced by R7 $\Delta$ 60 and R7f $\Delta$ 60 relative to R7 and R7f, respectively, was due to the reduced transforming activities of the R7 $\Delta$ 60 and R7f $\Delta$ 60 Gag-tMos proteins.

The present study further demonstrated that the insertion of FLAG did not significantly reduce the transforming activities of R7f, R7f $\Delta$ 60, or R7f $\Delta$ 447 in NIH/3T3 cells. Nevertheless, the insertion of FLAG reduced the brain lesion-inducing ability of R7f and R7f $\Delta$ 60 by approximately 50% compared with that of their FLAG-less counterparts. As previously argued, it appears that the insertion of the FLAG residues reduced the transforming ability of the Gag-tMos proteins, although the NIH/3T3 cell focus-forming assay was insufficiently sensitive to discern the difference.

The data presented in this report indicate that the entire R7 *gag* sequence is required for induction of brain lesions in 100% of infected mice. We have previously shown that SV7d1, containing the same genetic background as R7 except for the possession of the MoMuSV124 *env-mos* rather than the *gag-tmos* gene, also induces brain lesions in all injected mice. Consequently, the Gag residues of the R7 Gag-tMos protein may be substituted with the N-terminal 68 residues of MoMuSV124 Env-Mos protein without affecting the brain lesion-inducing

potential of the Mos protein. Interestingly, the present study demonstrated that R7Δ226 (whose Gag-tMos N-terminal sequence consists of 86 Gag residues) induced brain lesions in only 48% of injected mice, whereas SV7d1 (whose Env-Mos N-terminal sequence is a comparable length, 68 residues) induces brain lesions in all injected mice (Lim *et al*, 2000). This observation indicates that the specific residues of the wild-type v-Mos N-terminal sequence are more efficient at inducing brain lesions. Taken together, the above findings suggest that the length and unique composition of the R7 or SV7d1 N-terminal sequences appear to be optimized for interaction with the rest of the Mos protein thus enabling the respective Mos proteins to phosphorylate specific substrates leading to brain lesion induction. The basis for this optimization remains to be determined. Likewise, it remains to be determined how the insertion of the FLAG residues reduces the brain lesion-inducing potential of Mos. Until the crystal structure of Mos is solved, it will be difficult to propose a model that accurately represents how the N- and C-termini affect Mos structure and function. Still, in light of the crystal structure of other kinases (Knighton *et al*, 1991a,b; Hubbard *et al*, 1994), one might speculate that the length and conformation assumed by the residues at the N- and C-termini may either cover or expose the active site, which in turn may alter kinase activity directly or indirectly by preventing the binding or reducing the binding affinity of specific substrates.

In conclusion, we have demonstrated for the first time that altering the structure of a Mos protein can affect disease manifestation. In particular, our findings indicate that the entire *gag* sequence of the R7 Gag-tMos protein is required for efficient brain lesion induction and that addition to its C-terminus reduces the brain lesion-inducing ability of R7.

## Materials and methods

### Cell culture

Mouse NIH/3T3 fibroblasts and Ψ2 packaging cells (Mann *et al*, 1983) were cultured and maintained as previously described (Yuen *et al*, 1991).

### Virus strains

R7 is a spontaneous deletion mutant of SV7, a molecular clone of MoMuSV124 (Soong *et al*, 1984; Yuen *et al*, 1991; Yuen and Kwak, 1997). Compared with the MoMuSV124 genome, the 3401-bp R7 genome (Figure 1) is missing 2591 bp including 217 bp of the 3' end of the p15 coding sequence, all of the p12 coding sequence, all of the p30 coding sequence except for the central 263 bp, all of p10 and the *pol* coding sequence, the 15 bp *env* N-terminal sequence, and 203 bp of the 5' end of the *mos* gene (Yuen and Kwak, 1997). The TB strain of Moloney murine leukemia virus (MoMuLV-TB) was

used as the helper virus. MoMuLV-TB is a variant of MoMuLV (Yuen *et al*, 1985) whose genome differs from that of the standard MoMuLV (Szurek *et al*, 1988; Yuen and Szurek, 1989). MoMuLV-TB is less virulent than MoMuLV and induces T-cell lymphomas at 4–9 months postinoculation (Yuen and Szurek, 1989).

### PCR amplification

PCR amplification was performed as previously described (Yuen and Kwak, 1998). PCR primers (Table 4) were synthesized and purified by ethanol precipitation by Ransom Hill Bioscience (Ramona, CA, USA).

### DNA sequencing

Automated and manual DNA sequencing was performed at either The University of Texas at Austin Sequencing Facility or The University of Texas M.D. Anderson Cancer Center Science Park – Research Division (Smithville, TX, USA).

### Construction of mutants R7Δ60 and R7Δ226

R7Δ60 and R7Δ226 were constructed by cleaving pR7, a plasmid containing the complete linear R7 genome (Yuen and Kwak, 1997), at its unique *Xho*I<sub>1457</sub> site; digesting the cleaved ends with Bal 31 nuclease (Gibco-BRL, Gaithersburg, MD, USA); filling in the overhangs; and religating the molecules. R7Δ60 had 60 bp deleted from the p30 coding sequence extending from R7 bp 1458 to 1517 (inclusive) (Figure 1, line 2). R7Δ226 had a 226-bp deletion spanning R7 bp 1374 to 1599 (inclusive) that removed 183 bp of p30, the 6-bp R7 *gag-mos* junction sequence, the 7-bp insert, and the first 30 bp of the R7 *tmos* gene (Figure 1, lines 1 and 4) (Yuen and Kwak, 1997).

### Construction of R7f and its gag deletion mutants

The FLAG sequence encoding the octapeptide N-Asp-Tyr-Lys-Asp-Asp-Asp-Lys-C was inserted at the 3' end of R7 *tmos*, immediately before the stop codon (Figure 2). First, primers ms51 and FR, which contains the FLAG sequence (Table 4), were used to amplify the *mos* sequence extending from R7 bp 997 to the *Hind*III<sub>2515</sub> site at the end of the *mos* gene; pR7 served as the template. The amplified PCR product was then digested with *Nsi*I<sub>1659</sub> and *Hind*III<sub>2515</sub> and purified. The *Nsi*I<sub>1659</sub>–*Hind*III<sub>2515</sub> fragment extended from the third Met codon of the *mos* gene to the 3' end of *mos* including the FLAG sequence and the stop codon. This fragment was then exchanged with the homologous sequence in pR7 to generate pR7f. The incorporation of the FLAG sequence was verified by sequencing the ms34as-ms52as PCR-amplified product.

The FLAG-tagged *gag* deletion mutants were generated by exchanging the FLAG-tagged *Nsi*I–*Hind*III fragment with the homologous sequence in the pool of Bal-31-treated pR7 DNA. The resulting

DNA was electroporated into NIH/3T3 cells as previously described (Yuen *et al*, 1991; Yuen and Kwak, 1997). Several transformed foci were purified by single-cell cloning. The sequence spanning the deletion of several deletion mutants was determined by sequencing individually amplified PCR products using primers ms51 and ms32. R7fΔ60, R7fΔ192, and R7fΔ447 were obtained from the pool of Bal 31-treated DNA. R7fΔ60, with 60 bp of the *gag* sequence deleted from its genome, was genetically identical to R7Δ60 (Figure 1, line 2), except for the presence of the FLAG sequence and removal of 24 bp 3' to the stop codon (Figure 2). R7fΔ192 had a 192-bp sequence deletion extending from bp 1367 to 1558 (inclusive) (Figure 1, line 3), which removed 190 bp of p30 and the first 2 bp of the R7 *gag-tmos* junction sequence (Yuen and Kwak, 1997). R7fΔ447 had 447 bp deleted extending from bp 1141 to 1587 (inclusive) (Figure 1, line 5). The R7fΔ447 deletion encompassed 153 bp of p15, all 263 bp of p30, the 6-bp R7 *gag-tmos* junction sequence, the 7-bp insert, and the first 18 bp of the R7 *tmos* gene (Yuen and Kwak, 1997).

#### Construction of R7Δ447

The region spanning the 447-bp deletion in R7fΔ447 was PCR amplified with the primer set L5-ms32 and the cellular DNA of an R7fΔ447-producing cell line as template. The amplified fragment was digested with *AatII*<sub>888</sub> and *NsiI*<sub>1659</sub>, which encompasses the R7fΔ447 deletion. The purified *AatII*<sub>888</sub>–*NsiI*<sub>1659</sub> fragment was then exchanged with the corresponding region in pR7. Sequence analysis verified that the genome of R7Δ447 was identical to that of R7fΔ447 (Figure 1) except for the insertion of the FLAG sequence and the deletion of the 24 bp immediately 3' of the *mos* stop codon (Figure 2).

#### Construction of R7fΔgag

Plasmid pR7fΔgag was constructed by first generating pR7ltrs, a pSP72 vector (Promega, Madison, WI, USA) containing the *Clal*–*PstI* fragment consisting of the R7 3' noncoding sequence, the 5' LTR, and the 5' noncoding sequence extending to the *PstI*<sub>1064</sub> site, linked via a 16 bp pSP72 polylinker to the *HindIII*–*PstI* fragment consisting of the 3' noncoding sequence and 3' LTR and 5' noncoding sequence (Yuen and Kwak, 1997). To generate pR7fΔgag, the 958 bp *HindIII*<sub>1558</sub>–*HindIII*<sub>2515</sub> fragment of pR7f containing only the 7-bp R7 insert and the FLAG-tagged *tmos* coding sequence was inserted into pR7ltrs at the *HindIII* site (Figure 1, line 6). The splice junction between the 5' noncoding sequence and *tmos* was confirmed by sequence analysis.

#### Electroporation of genomic DNA

Electroporation of genomic DNA into Ψ2 or NIH/3T3 cells was performed as previously described (Yuen *et al*, 1991).

#### Virus rescue

Each cell line was superinfected with MoMuLV-TB at an m.o.i. of 1 to rescue the replication-defective *mos*-containing (sarcoma) viruses. Although supernatants containing the defective sarcoma viruses and MoMuLV-TB were used throughout this study, only the sarcoma virus is noted in this report, unless specified otherwise.

#### Transforming activity

The transforming activity of the sarcoma viruses produced by cell lines chronically infected with MoMuLV-TB and R7 (or one of its mutants) was determined by seeding 60-mm dishes with chronically infected NIH/3T3 cells. At subconfluence, the medium was replaced with 5 ml fresh medium. Twenty-four hours later, the supernatant was harvested and filtered through a 0.45-μm membrane filter. The total number of cells in each plate was also counted. The number of focus-forming sarcoma particles in the supernatant was determined using the NIH/3T3 cell focus forming assay as previously described (Wong *et al*, 1981). The number of focus-forming units (FFUs) reported herein represent the mean number of FFUs produced by several chronically infected cell lines during a 24-h period and normalized to 10<sup>6</sup> cells/ml of supernatant. The transforming activity of the sarcoma viruses produced in *de novo* infections was also determined by seeding 1 × 10<sup>5</sup> NIH/3T3 cells in 60-mm dishes and infecting the cells at an m.o.i. of 5. Three days later, the supernatant was replaced with 5 ml fresh medium. The supernatant was then harvested and assayed as described above for supernatants harvested from chronically infected cells. The transforming activity of each virus was assayed at least twice.

#### Isolation of total cellular RNA and viral RNA and Northern blotting

Extraction and fractionation of total cellular RNA were performed as previously described (Yuen and Kwak, 1998). To isolate RNA from virus particles, 225 ml of supernatant were harvested from R7fΔgagSc1 cells coinfecting with MoMuLV-TB and filtered through a 0.8-μm filter. Virus particles were pelleted by ultracentrifugation at 30 000 r.p.m. at 4°C for 1 h. Lysis and extraction of RNA from the pelleted particles were performed using the RNeasy Mini Kit (Qiagen, Valencia, CA, USA). Northern blotting was performed as described (Yuen and Kwak, 1998). A 909-bp *BglI*<sub>3669</sub>–*HindIII*<sub>4578</sub> fragment from MoMuSV124 was gel purified, labeled with α-<sup>32</sup>P, and used as a probe.

#### Protein extraction

NIH/3T3 cells were seeded at 6 × 10<sup>5</sup> cells/100-mm plate and infected with the respective viruses at an m.o.i. of 5. Cells were washed in TBS (20 mM Tris-HCl [pH 7.6], 137 mM NaCl) and lysed with 0.5 ml

of lysis buffer (1% NP-40, 150 mM NaCl, 1 mM EDTA, 2 mM dithiothreitol [DTT], 0.2 trypsin inhibitor units/ml aprotinin, 1 mM phenylmethylsulfonyl fluoride, and 2  $\mu$ g/ml leupeptin). Lysates were precleared overnight at 4°C with 100  $\mu$ l of Pansorbin cells (Calbiochem-Novabiochem Corporation, La Jolla, CA, USA), quantitated using a Bio-Rad DC Protein Assay Kit (Bio-Rad Laboratories, Hercules, CA, USA), aliquoted, and stored at -80°C until used.

#### Western blotting

Aliquots of each protein were fractionated by 9% reducing sodium dodecyl sulfate-polyacrylamide gel electrophoresis (SDS-PAGE), transferred to Hybond-P PVDF membranes (Amersham, Little Chalfont, UK) by semi-dry blotting, and blocked with 5% skim milk in TBS containing 0.1% Tween-20 (TBS-T). Each membrane was incubated with 2  $\mu$ g/ml primary M2 antibody (Sigma, St. Louis, MO, USA) or CasBrMLV p15 monoclonal antibody (gift from Dr J Portis) for 1 h at room temperature followed by 1 h of incubation with a 1:50 000 dilution of peroxidase-labeled antibody to mouse IgG (Sigma, St. Louis, MO, USA). Antibodies were diluted in TBS-T containing 1% bovine serum albumin (Sigma, St. Louis, MO, USA). Proteins were visualized using the ECL Plus detection kit and exposure to Hyperfilm ECL (Amersham, Little Chalfont, UK), according to the manufacturer's recommendations. In all gels, a broad-range biotinylated protein marker (Bio-Rad, Hercules, CA, USA) was coelectrophoresed, transferred to Hybond-P membrane, probed with Streptavidin-HRP conjugate (Gibco-BRL, Gaithersburg, MD, USA), and visualized as described above.

#### Histopathology

Intraperitoneal injection of virus into BALB/c mice, necropsy of diseased mice, and preservation and processing of organs for histopathology were performed as previously described (Yuen *et al*,

1991; Yuen and Kwak, 1998). BALB/c mice less than 48 h old were injected intraperitoneally with FFUs in the ranges indicated in Tables 2 and 3. Infected mice were killed and necropsied when they became moribund. Mice exhibiting no physical abnormalities were killed and necropsied at 60–65 d.p.i. Brain lesions (i.e., dark red spots on whole brains) visible to the naked eye or through an 8 $\times$  magnifying lens were counted. Microscopic examination of brain sections confirmed that the dark red spots were brain hemorrhages or angioendotheliomas.

#### Statistical analysis

The statistical significance of differences in transforming activity exhibited by R7, R7f, and their *gag* deletion mutants was determined by one-way analysis of variance. The number of FFUs detected was log<sub>10</sub> transformed to stabilize the variance. Differences were considered significant when  $P < 0.001$ . The statistical significance of the incidence of brain lesions was determined by chi square analysis. Fisher's exact test was used when the expected frequencies were less than 1.

#### Acknowledgments

We thank Sean Hensley and Dr Jianjun Shen of the Molecular Core at UT M.D. Anderson Cancer Center-Science Park and The University of Texas at Austin Sequencing Facility for DNA sequencing. We also thank Judy Ing for assistance with the artwork, Dr Dennis Johnston for statistical analysis, Dr Youn-Tae Kwak for assistance with the constructs, Dr Esther Ryan for assisting in the pathological studies, and Helen Zhang for technical assistance. Part of the sequencing was supported by grant number ES07784 from the National Institute of Environmental Health Sciences.

#### References

- Berman LD, Allison AC (1969). Studies on murine sarcoma virus: a morphological comparison of tumorigenesis by the Harvey and Moloney strains in mice, and the establishment of tumor cell lines. *Int J Cancer* **4**: 820–836.
- Chirigos MA, Scott D, Turner W, Perk K (1968). Biological, pathological and physical characterization of a possible variant of a murine sarcoma virus (Moloney). *Int J Cancer* **3**: 223–227.
- Gallick GE, Sparrow JT, Singh B, Maxwell SA, Stanker LH, Arlinghaus RB (1985). Recognition of mos-related proteins with an antiserum to a peptide of the v-mos gene product. *J Gen Virol* **66**: 945–955.
- Gazdar AF, Chopra HC, Sarma PS (1972). Properties of a murine sarcoma virus isolated from a tumor arising in an NZW-NZB F 1 hybrid mouse. I. Isolation and pathology of tumors induced in rodents. *Int J Cancer* **9**: 219–233.
- Hayashi Y, Tange T, Urano Y, Smadja-Joffe F, Le Bousse-Kerdiles MC, Jasmin C (1988). Histopathologic studies on myeloproliferative sarcoma virus (MPSV) induced leukemias and hemangiosarcoma in Jar-2 rats. *Pathol Res Pract* **183**: 314–320.
- Herzog NK, Nash M, Ramagli LS, Arlinghaus RB (1990). v-mos protein produced by in vitro translation has protein kinase activity. *J Virol* **64**: 3093–3096.

- Hubbard SR, Wei L, Ellis L, Hendrickson WA (1994). Crystal structure of the tyrosine kinase domain of the human insulin receptor [see comments]. *Nature* **372**: 746–754.
- Knighton DR, Zheng J, Ten Eyck LF, Ashford VA, Xuong NH, Taylor SS, Sowadski JM. (1991a). Crystal structure of the catalytic subunit of cyclic adenosine monophosphate-dependent protein kinase. *Science* **253**: 407–414.
- Knighton DR, Zheng J, Ten Eyck LF, Xuong NH, Taylor SS, Sowadski JM (1991b). Structure of a peptide inhibitor bound to the catalytic subunit of cyclic adenosine monophosphate-dependent protein kinase. *Science* **253**: 414–420.
- Kozak M (1987). An analysis of 5'-noncoding sequences from 699 vertebrate messenger RNAs. *Nucleic Acids Res* **15**: 8125–8148.
- Le Bousse-Kerdiles MC, Smadja-Joffe F, Klein B, Caillou B, Jasmin C (1980). Study of a virus-induced myeloproliferative syndrome associated with tumor formation in mice. *Eur J Cancer* **16**: 43–51.
- Lim KY, Ryan EA, Wong PKY, Yuen PH (2000). Studies on the pathology, especially brain hemorrhage and angioendotheliomas, induced by two new *mos*-containing viruses. *J NeuroVirology*, **6**, (in press).
- Mann R, Mulligan RC, Baltimore D (1983). Construction of a retrovirus packaging mutant and its use to produce helper-free defective retrovirus. *Cell* **33**: 153–159.
- Moloney JB (1966). A virus-induced rhabdomyosarcoma of mice. *Natl Cancer Inst Monogr* **22**: 139–142.
- Ostertag W, Vehmeyer K, Fagg B, Pragnell IB, Paetz W, Le Bousse MC, Smadja-Joffe F, Klein B, Jasmin C, Eisen H (1980). Myeloproliferative virus, a cloned murine sarcoma virus with spleen focus-forming properties in adult mice. *J Virol* **33**: 573–582.
- Perk K, Moloney JB (1966). Pathogenesis of a virus-induced rhabdomyosarcoma in mice. *J Natl Cancer Inst* **37**: 581–599.
- Propst F, Cork LC, Kovatch RM, Kasenally AB, Wallace R, Rosenberg MP (1992). Progressive hind limb paralysis in mice carrying a v-Mos transgene. *J Neuropathol Exp Neurol* **51**: 499–505.
- Propst F, Rosenberg MP, Cork LC, Kovatch RM, Rauch S, Westphal H, Khillan J, Schulz NT, Neumann PE, Newmann PE (1990). Neuropathological changes in transgenic mice carrying copies of a transcriptionally activated *Mos* protooncogene [published erratum appears in Proc Natl Acad Sci USA (1991) **88**: 4060.]. *Proc Natl Acad Sci USA* **87**: 9703–9707.
- Ribacchi R, Giraldo G (1966). Plasmacytomas occurring in the bones of rats injected intracerebrally with murine sarcoma virus (MSV), Moloney strain: preliminary report. *Lav Ist Anat Isotol Patol Perugia* **26**: 149–156.
- Simons PJ, McCully DJ (1970). Pathologic and virologic studies of tumors induced in mice by two strains of murine sarcoma virus. *J Natl Cancer Inst* **44**: 1289–1303.
- Soong MM, Yuen PH, Wong PK (1984). Isolation and characterization of a Mo-MuSV-transformed TB cell line that produces noninfectious MuSV particles with uncleaved gag protein which is processed in the presence of Mo-MuLV. *Virology* **132**: 390–400.
- Stanton MF, Law LW, Ting RC (1968). Some biologic, immunogenic, and morphologic effects in mice after infection with a murine sarcoma virus. II. Morphologic studies. *J Natl Cancer Inst* **40**: 1113–1129.
- Stoica G, Hoffman J, Yuen PH (1990). Moloney murine sarcoma virus 349 induces Kaposi's sarcomalike lesions in BALB/c mice. *Am J Pathol* **136**: 933–947.
- Szurek PF, Yuen PH, Jerzy R, Wong PK (1988). Identification of point mutations in the envelope gene of Moloney murine leukemia virus TB temperature-sensitive paralytogenic mutant ts1: molecular determinants for neurovirulence. *J Virol* **62**: 357–360.
- Wong PK, Soong MM, Yuen PH (1981). Replication of murine leukemia virus in heterologous cells: interaction between ecotropic and xenotropic viruses. *Virology* **109**: 366–378.
- Yuen PH, Kwak YT (1997). R7, a spontaneous mutant of Moloney murine sarcoma virus 124 with three direct repeats and an in-frame truncated gag-mos gene, induces brain lesions. *Virology* **236**: 213–218.
- Yuen PH, Kwak YT (1998). Studies on the pathology, especially brain lesions, induced by R7, a spontaneous mutant of Moloney murine sarcoma virus 124. *Am J Pathol* **152**: 1509–1520.
- Yuen PH, Malehorn D, Nau C, Soong MM, Wong PK (1985). Molecular cloning of two paralytogenic, temperature-sensitive mutants, ts1 and ts7, and the parental wild-type Moloney murine leukemia virus. *J Virol* **54**: 178–185.
- Yuen PH, Matherne CM, Molinari-Storey LM (1991). SV7, a molecular clone of Moloney murine sarcoma virus 349, transforms vascular endothelial cells. *Am J Pathol* **139**: 1449–1461.
- Yuen PH, Szurek PF (1989). The reduced virulence of the thymotropic Moloney murine leukemia virus derivative MoMuLV-TB is mapped to 11 mutations within the U3 region of the long terminal repeat. *J Virol* **63**: 471–480.